C. R. Mecanique 340 (2012) 120–129

Contents lists available at SciVerse ScienceDirect

Comptes Rendus Mecanique

www.sciencedirect.com

Limit analysis of hollow spheres or spheroids with Hill orthotropic matrix

Analyse limite et modèle de la sphère ou du sphéroïde creux à matrice anisotrope de Hill

Franck Pastor [a], Joseph Pastor [b], Djimedo Kondo [c,*]

[a] *Laboratoire de mécanique de Lille, UMR 8107 CNRS, université de Lille 1, cité scientifique, 59655 Villeneuve d'Ascq, France*
[b] *Laboratoire LOCIE, UMR 5271 CNRS, université de Savoie, 73376 Le Bourget du Lac, France*
[c] *Université Pierre-et-Marie-Curie, institut D'Alembert, UMR 7190 CNRS, 4, place Jussieu, 75252 Paris cedex 05, France*

ARTICLE INFO

Article history:
Received 15 October 2011
Accepted after revision 28 November 2011
Available online 7 February 2012

Keywords:
Porous media
Anisotropy
Hill matrix
Gurson approach
Hollow spheroid model
Limit analysis
3D-FEM
Conic optimization

Mots-clés :
Mileux poreux
Anisotropie
Matrice de Hill
Approche Gurson
Modèle du sphéroïde creux
Analyse limite
3D-MEF
Optimization conique

ABSTRACT

Recent theoretical studies of the literature are concerned by the hollow sphere or spheroid (confocal) problems with orthotropic Hill type matrix. They have been developed in the framework of the limit analysis kinematical approach by using very simple trial velocity fields. The present Note provides, through numerical upper and lower bounds, a rigorous assessment of the approximate criteria derived in these theoretical works. To this end, existing static 3D codes for a von Mises matrix have been easily extended to the orthotropic case. Conversely, instead of the non-obvious extension of the existing kinematic codes, a new original mixed approach has been elaborated on the basis of the plane strain structure formulation earlier developed by F. Pastor (2007). Indeed, such a formulation does not need the expressions of the unit dissipated powers. Interestingly, it delivers a numerical code better conditioned and notably more rapid than the previous one, while preserving the rigorous upper bound character of the corresponding numerical results. The efficiency of the whole approach is first demonstrated through comparisons of the results to the analytical upper bounds of Benzerga and Besson (2001) or Monchiet et al. (2008) in the case of spherical voids in the Hill matrix. Moreover, we provide upper and lower bounds results for the hollow spheroid with the Hill matrix which are compared to those of Monchiet et al. (2008).

© 2011 Published by Elsevier Masson SAS on behalf of Académie des sciences.

RÉSUMÉ

De récentes études dans la littérature ont porté sur l'établissement de critères macroscopiques de milieux plastiques orthotropes de type Hill contenant des vides sphériques ou sphéroïdaux. Pour évaluer ces critères, nous avons étendu les codes statiques et cinématiques 3D existants du cas isotrope à l'anisotrope. Les codes statiques ont pu l'être assez aisément, l'approche cinématique étant plus problématique du fait des indispensables discontinuités de vitesses. Pour cette raison une nouvelle et originale approche mixte a donc été élaborée sur la base de la formulation proposée par F. Pastor (2007) pour les structures en déformation plane, cette formulation ayant l'avantage de ne pas nécessiter l'expression des puissances dissipées unitaires. Cette approche mixte a débouché sur un code mieux conditionné et significativement plus rapide que le code précédent, sans perdre pour autant le caractère de borne supérieure rigoureuse du résultat. La pertinence de la nouvelle approche a été d'abord démontrée sur le cas d'une matrice de von Mises, obtenu comme cas particulier de la matrice de Hill. Puis, des bornes numériques sont fournies et

* Corresponding author.
E-mail addresses: franck.pastor@univ-lille1.fr (F. Pastor), joseph.pastor@univ-savoie.fr (J. Pastor), djimedo.kondo@upmc.fr (D. Kondo).

1631-0721/$ – see front matter © 2011 Published by Elsevier Masson SAS on behalf of Académie des sciences.
doi:10.1016/j.crme.2011.11.011

comparées au critère établi par Benzerga et Besson (2001) et Monchiet et al. (2008) dans le cas de la matrice orthotrope avec une cavité sphérique. Enfin, les prédictions de Monchiet et al. (2008) dans le cas d'une cavité sphéroïdale plongée dans la matrice orthotrope sont évaluées et discutées.

© 2011 Published by Elsevier Masson SAS on behalf of Académie des sciences.

1. Introduction

The well-known Gurson [1] isotropic criterion of ductile porous media has been obtained by studying a hollow sphere with a von Mises rigid plastic matrix subjected to uniform strain rate boundary conditions. Gurson's analysis consisted in the use of a kinematic approach of limit analysis (LA) to obtain an upper bound to the exact macroscopic criterion for isotropic porous materials. Later, following the kinematic limit analysis approach, several extensions of the Gurson criterion, mainly accounting for void-shape effects, have been proposed (see among others [2–6]). Effects of plastic anisotropy of the matrix have been addressed first in [7] for spherical voids, and later in the case of spheroidal (prolate and oblate) voids by [8] and then [9]. For a detailed review on these developments, the reader is referred to [10]. A common aspect of the theoretical studies dealing with orthotropic matrix is that they are all based on relatively simple trial velocity fields, largely inspired from the isotropic case. Only few comparisons with cell calculation by means of finite elements are available in [9].

On the other hand, using finite element discretization of mechanical systems, original static and kinematic LA methods made it possible to obtain rigorous lower and upper bounds allowing to control Gurson's kinematic approaches for cylindrical cavities [11,12]. In the axisymmetric and 3D study of [13] the Gurson criterion appears to be satisfactory for materials with spherical cavities, although without taking into account the influence of third stress invariant as in [14].

Very recently, first investigations on ductile materials with oblate cavities in an isotropic von Mises matrix have been done in the short paper [15]; in [16] are fully detailed the theoretical criteria and the numerical methods and their application to both cases of prolate and oblate cavities, providing rigorous assessment of existing theoretical models of ductile porous materials with spheroidal voids. In all the codes, the mechanical problem has been cast as a conic programming problem solved by the very effective commercial code MOSEK [17].

The objective of the present paper is to provide numerical upper and lower bounds of the macroscopic criteria of porous media having Hill orthotropic matrix [18]. The study focused first on the extension of the existing codes to the case of the anisotropic matrix. For the static limit analysis approach, the static codes have been easily modified by mean of a simple change of variables. This it not the case for the kinematic approach, mainly because of the velocity discontinuities allowed through any tetrahedron side. To overcome this difficulty, we have extended to the 3D homogenization problem the mixed formulation defined in [19] and applied to plane strain structures in von Mises and Gurson materials (see [20]). Indeed, this mixed formulation requires only the plasticity criterion of the material, without any recourse to the expression of the unit dissipated power as in the direct kinematic method used in [15] in the isotropic case. For comparison purpose, both resulting codes are first applied to the Gurson problem for validation and comparison with previous results in the von Mises matrix case. Then, owing to the good performance of the new codes, we provide numerical upper and lower bounds of the macroscopic criterion in the case of hollow sphere and spheroid with a Hill orthotropic matrix. This allows to assess the recent corresponding theoretical criteria available in the literature.

2. Formulation of the mixed kinematic approach of limit analysis

2.1. Brief recall of limit analysis

In this section, the basic principles of limit analysis theory are briefly recalled. According to [21], a stress tensor field, σ, is said to be admissible if it is both statically admissible (SA) (i.e., satisfies equilibrium equations, stress vector continuity, and stress boundary conditions) and plastically admissible (PA), i.e., $f(\sigma) \leqslant 0$, where $f(\sigma)$ is the local convex yield function.

Similarly, a strain rate tensor field, d, is admissible if it is both kinematically admissible (KA, i.e., it derived from a piecewise continuous velocity vector field u, with bounded discontinuities $[u]$, such that the velocity boundary conditions are fulfilled) and plastically admissible (PA), i.e., the following associated flow rules (1.i), (1.ii) are satisfied:

$$d = \lambda \frac{\partial f}{\partial \sigma}, \qquad \lambda f(\sigma) = 0, \qquad \lambda \geqslant 0, \quad f(\sigma) \leqslant 0 \tag{1.i}$$

$$[u] = \xi \frac{\partial f_{nt}}{\partial T}, \qquad \xi f_{nt}(T) = 0, \qquad \xi \geqslant 0, \quad f_{nt}(T) \leqslant 0 \tag{1.ii}$$

where $[u]$ is the velocity jump across the discontinuity surfaces, and T the corresponding stress vector acting on them. The criterion $f_{nt}(T)$ results from the projection of the plasticity criterion $f(\sigma)$ on the Mohr plane, where n is the normal to the element of the velocity discontinuity surface and $T = (\sigma_{nn}, \sigma_{nt_1}, \sigma_{nt_2})$ is the stress vector on this element on which an orthonormal frame (n, t_1, t_2) is defined.

It is worth noting that, if (1.i) and (1.ii) are fulfilled, the quantities $\sigma : d$ and $T \cdot [u]$ become, respectively, the *convex* unit dissipated powers $\pi_{vol}(d)$ and $\pi_{disc}([u])$, i.e.:

$$\pi_{vol}(d) = \sigma : d, \qquad \pi_{disc}\big([u]\big) = T \cdot [u] \tag{2}$$

Let us assume that the virtual power of the external loads P_{ext} can be written as the scalar product of a load vector $Q = Q(\sigma)$ (with σ SA), and a generalized velocity vector $q = q(u)$ (with u KA). The p components of Q and q are called loading and kinematic parameters, respectively. The virtual power principle reads:

$$P_{\text{ext}} = Q \cdot q = \int_V \sigma : d \,\mathrm{d}V + \int_{S_d} T \cdot [u] \,\mathrm{d}S \tag{3}$$

where V is the volume of the mechanical system, and S_d the set of the velocity discontinuity surfaces.

A solution of the LA problem is a pair (σ, u) where σ and u are both admissible fields and associated by the normality rule. In this case, the loading vector corresponding to the field σ is a limit load Q_{lim} of the mechanical system. The admissible loads Q belong to a set K whose boundary ∂K is the locus of the limit loads Q_{lim}. Classically, the limit loads can be found or approached using two dual optimization methods. The first one is the static method which is in terms of admissible stresses and leads to a lower bound of the limit loads.

The second method, involving only the displacement velocities as variables, is the classical kinematic (or upper bound) method. Let us assume that the velocity field u is q^d-admissible, i.e., u is admissible and verify $q(u) = q^d$, where q^d is a fixed value of q. The classical kinematic approach of LA consists in solving the following minimization problem, for various values of q_d:

$$Q \cdot q_d = \min_{q^d\text{-admissible } u} \left(\int_V \pi_{vol}\big(d(u)\big) \,\mathrm{d}V + \int_{S_d} \pi_{disc}\big([u]\big) \,\mathrm{d}S \right) \tag{4}$$

As a consequence, the classical method needs the analytical expressions of the unit dissipated powers $\pi_{vol}(d)$ and $\pi_{disc}([u])$. From a numerical point of view, these expressions must be taken into account without difficulty when using optimization algorithms. But this is not so easy in the case of an anisotropic matrix when out-of-axis discontinuities are present as here. For this reason, a kinematical mixed formulation is investigated by extending the formulation of [19,20]. By doing so, only the plasticity criterion is required as in the static code.

2.2. Formulation of the mixed kinematic problem to be solved

Let us now consider a KA virtual velocity field u. The virtual power principle (VPP) states that the stress tensor fields σ and the load vector Q are in equilibrium if, *for any KA* u, Eq. (3) is verified. The mixed formulation of [19] and [20] can be modified as:

$$\max_{Q,\sigma,\sigma'} F = Q \cdot q_d \tag{5.i}$$

$$\text{s.t.} \quad \int_V \sigma : d \,\mathrm{d}V + \int_{S_d} \big(\sigma' \cdot n\big) \cdot [u] \,\mathrm{d}S = Q \cdot q(u) \quad \forall \text{KA } u \tag{5.ii}$$

$$f(\sigma) \leqslant 0, \quad f\big(\sigma'\big) \leqslant 0 \tag{5.iii}$$

where σ is a PA stress tensor inside the 3D finite elements, and σ' another PA stress tensor along the discontinuity surfaces. The main advantage of this formulation is that the plasticity criterion $f(\sigma')$ can be written in the anisotropy axes taken as the global axes, instead of the local axes.

The previous formulation gives the exact solution if any velocity and stress fields could be taken into account. This is not always the case when we consider a discretization of the mechanical system in finite elements, giving in fact only estimates of the limit loads. Then, to preserve the rigorous kinematical character of the final result, we will need to modify the numerical implementation of the virtual power principle (5.ii) on the basis of convexity properties when taking into account the contribution of the discontinuities.

The mechanical 3D hollow spheroid is discretized in tetrahedrons as presented in [15] (or in [13] for the Gurson problem), with displacement velocities as virtual variables and independent stress tensors as real variables. First, we examine the contribution of the continuous velocity fields to the VPP expression (3); the role of the inter-element discontinuities will be analyzed in the next subsection.

2.3. Numerical contribution of the element velocity fields

A three-component nodal vector $\{u\}$ is located at each apex of the tetrahedron, and the velocity u is assumed to vary linearly, giving rise to a constant strain rate $\{d\}$ in the element. Then, a single stress tensor $\{\sigma\}$ is assigned at each tetrahedron. Thus, from its definition, the external power reads:

$$P_{\text{ext}} = q(u)\cdot Q = \{q(u)\}^T\{Q\} = \{u\}^T[\beta]\{Q\} \tag{6}$$

where $[\beta]^T$ is the matrix resulting from the calculation of the generalized velocity $q(u)$.

Inside the element k, the strain rate $\{d\}$ is defined by the classical equation:

$$\{d\}_k = [B]_k\{u^n\} \tag{7}$$

where the vector $\{u^n\}$ collects the twelve degrees of freedom of the element. Then the VPP (3) reads:

$$\{q(u)\}^T\{Q\} = \sum_k V_k\big[\{d\}_k^T\{\sigma\}\big] \quad \forall \text{KA } u \tag{8}$$

where V_k denotes the volume of the tetrahedron k. Using Eq. (7), and after the assembly of the elements, the relationship (8) gives rise to the following variational system:

$$\{u\}^T\big[-[\alpha]\{\sigma\} + [\beta]\{Q\}\big] = 0 \quad \forall \text{KA } \{u\} \tag{9}$$

where the matrix $[\alpha]$ results from the assembly of the submatrices $[\alpha] = V_k[B^T]$ calculated for each element k in (8).

2.4. Numerical contribution of the velocity discontinuities

According to [22], a discontinuity surface element (of normal n) can be assimilated to a thin zone where the appropriate static and kinematic variables are respectively, in mathematical notation, the stress vector T' and the velocity jump vector $[u]$ associated by the normality law relatively to the $f_{nt}(T')$ criterion. The second left hand side term of (5.ii) becomes the dissipated power π_{disc} when the optimal solution is reached (see [19,20]), so we can use the convexity of π_{disc} since the velocity jump varies linearly along the discontinuity side. Hence an auxiliary stress tensor σ' is assigned at each apex i, j, m of the triangular discontinuity side S_{ijm}, and the integral on this side can be upper bounded by writing:

$$\int_{S_{ijm}} \big(\sigma'\cdot n\big)\cdot[u]\,\mathrm{d}S \leqslant A_{ijm}\big(\{[u]\}_i^T\big[\sigma_i'\big]\{n\} + \{[u]\}_j^T\big[\sigma_j'\big]\{n\} + \{[u]\}_m^T\big[\sigma_m'\big]\{n\}\big)/3 \tag{10}$$

where A_{ijm} is the area of S_{ijm} whose the normal is n. Using these bounds gives rise to a matrix $[\alpha']$ in an analogous manner than in the previous subsection.

Finally the resulting numerical form of the mixed problem (5) is the following:

$$\text{Max}\{q_d\}^T\{Q\} \tag{11.i}$$

$$\text{s.t.} \quad -[\alpha]\{\sigma\} - \big[\alpha'\big]\big\{\sigma'\big\} + [\beta]\{Q\} = 0 \tag{11.ii}$$

$$f(\sigma) \leqslant 0 \quad \forall\sigma, \qquad f\big(\sigma'\big) \leqslant 0 \quad \forall\sigma' \tag{11.iii}$$

$$+ \text{ KA velocity conditions} \tag{11.iv}$$

At this stage, it is worth recalling that the optimal velocities components are given by the values of the dual variables associated to the rows of the final matrix $[-\alpha, -\alpha', \beta]$, which are available in the optimal solution obtained with the code MOSEK or the interior point solver defined in [23] and intensively used in [19] and [20]. Now, to take into account numerically the KA and PA conditions, we need to explicit the homogenization problem which is the purpose of this Note. It is worth noting that there is no restriction to the allocated stress tensors, except the verification of the criterion; thus, for any non-zero velocity field (and the corresponding strain rates and velocity jumps) an associated PA stress tensor can be found. Consequently, from Hill's maximum work principle, the upper bound character is preserved with the above selected formulation.

3. Specific formulations of the considered homogenization problem

3.1. Formulation of the KA conditions

The present hollow spheroid problem, as in the Gurson one, is submitted to a uniform strain rate E at its boundary, i.e., at each of the apexes of the external boundary triangles of Fig. 1, the velocity must verify the Hill–Mandel condition $u_i = E_{ij}x_j$ (with $i, j = x, y, z$) where the z-axis here is the symmetry axis of the spheroid. Taking into account the objective of comparison with the desired results of the literature in terms of projection of the macroscopic criterion, we suppose that the strain rate tensor E is principal (as justified in [15]). Consequently, we can use the eighth of sphere in the positive octant of the (x, y, z) frame as in [15]. In Fig. 1 the mesh is made of n_{lay} layers of n_{div}^2 prisms (of triangular basis) discretized in 14 tetrahedrons each, with $n_{div} = 4$, $n_{lay} = 4$.

Hence we can define three supplementary lines (constraints) whose associated virtual variables are E_x, E_y, E_z (and three columns for the associated macroscopic stresses), so that the previous conditions read $u_x = E_x x$, $u_y = E_y y$, $u_z = E_z z$. Hence,

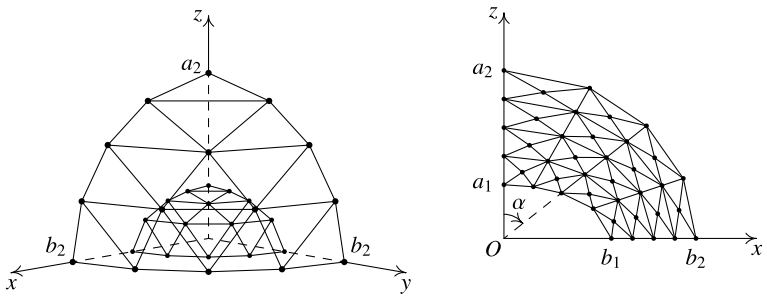

Fig. 1. General view and Oxz plane of an 896-tetrahedron mesh ($a_1/b_1 = 0.5,\ f = 0.1$).

for example for the first relation, in an additional column (located after those of the stresses and the Q_i) we initialize to 1 and $-x$ the components of the column corresponding to the virtual variable u_x and to the virtual variable E_x, respectively. Since this additional column does not appear in the functional, the desired relation will be verified in the optimal solution. This technique is in fact equivalent with the line condensation used in [20]. If the kinematic parameters are chosen as a linear invertible combination of E_x, E_y, E_z (represented by a non-singular square matrix A, for example), the above coefficients x, y, z are dispatched on the three additional lines according to the inverse of A.

A similar technique is used to impose the null symmetry values to the required velocity components of the planes $x = 0$, $y = 0$ and $z = 0$. This original technique gives rise to a better conditioning of the final matrix and avoids to have to renumber the rows when using the condensation technique.

3.2. Formulation of the PA conditions related to the Hill criterion

The Hill criterion, which is concerned with an orthotropic material of axis (x, y, z), reads:

$$\sqrt{F(\sigma_y - \sigma_z)^2 + G(\sigma_z - \sigma_x)^2 + H(\sigma_x - \sigma_y)^2 + 2L\sigma_{yz}^2 + 2M\sigma_{zx}^2 + 2N\sigma_{xy}^2} \leqslant \sigma_0\sqrt{2/3} \tag{12}$$

Since the orthotropy axes here are assumed to be the same as the (x, y, z)-axis and the loading E is principal, the above meshing and the symmetry conditions are justified. However, it is worth noting that neither the loading, nor the local fields are axisymmetric.

The criterion (12) can be easily written in the conic form $\sqrt{\sum_{j=1}^{6} x_j^2} \leqslant x_7 = \sigma_0\sqrt{2/3}$. In a similar manner as in [15], a change of variables $(\sigma_{ij} \to (\operatorname{tr}\sigma, x_2, \ldots, x_6))$ is operated in order to minimize the number of real and auxiliary variables of the numerical problem.

3.3. Formulation of the loading and kinematic parameters

Under the present Hill–Mandel boundary conditions, the virtual power principle classically reads:

$$P_{\text{tot}}/V = \Sigma_x E_x + \Sigma_y E_y + \Sigma_z E_z = Q \cdot q \tag{13}$$

For the next comparisons with the available results of the literature, i.e. the projection of the macroscopic criterion on the $(\Sigma_m, \Sigma_z - \Sigma_x)$ plane, the following loading and kinematic parameters are chosen:

$$Q_1 = \Sigma_m = \frac{1}{3}(\Sigma_x + \Sigma_y + \Sigma_z), \qquad Q_2 = \frac{\Sigma_z + \Sigma_x}{2} - \Sigma_y, \qquad Q_3 = \Sigma_z - \Sigma_x \tag{14}$$

$$q_1 = E_x + E_y + E_z, \qquad q_2 = \frac{2}{3}\left(\frac{E_z + E_x}{2} - E_y\right), \qquad q_3 = \frac{1}{2}(E_z - E_x) \tag{15}$$

It is worth noting that the above components are not in agreement with the geometric transverse isotropy (with z as the symmetry axis) resulting from the confocal spheroidal form of the matrix boundaries. This is not surprising since the further considered plastic matrix is orthotropic.

3.4. General comments

– In the present formulation, there is no need to impose the normality law (here the incompressibility) with additional constraints: the normality law is in fact automatically verified by the optimal solution. This property was pointed out from the plane strain numerical problem in [14] as a consequence of the Karush–Kuhn–Tucker optimality conditions, and the reasoning can easily be extended to the present 3D case. It was also proved in the same reference by a variational formulation of the general mechanical problem, thanks to an appropriate extension of the Radenkovic and Nguyen [24] presentation of the limit analysis problem.

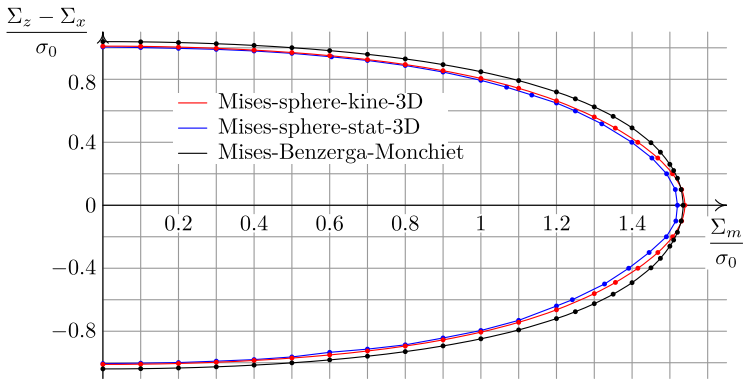

Fig. 2. Spherical void, von Mises matrix: comparison with the Gurson criterion, $f = 0.1$.

- Another advantage of the proposed mixed method concerns the better conditioning of the final numerical problem, owing to the fact that the real variables, here the stress components, are free of SA conditions and independent to one another. This feature implies that the constraint matrix is full-row rank, and no locking can occur as in the classical kinematic method, particularly with continuous velocity fields.
- A last advantage of the method is its easy applicability to any material obeying to other classical isotropic or anisotropic convex criteria, since only the expression of the criterion is needed. Hence, all the usual quadratic or conic criteria can be taken into account by modifying only the same part of both present static and kinematic codes; the resulting problems can be solved by using MOSEK as here, or with the help of a general convex code for non-polynomial criteria (for instance the Gurson one as in [20]).

4. Validation of the new codes and assessment of theoretical approximate criteria

We are looking for the projection of the macroscopic criterion $g_{hom}(\Sigma)$ on the plane $(Q_1 = \Sigma_m,\ Q_3 = \Sigma_z - \Sigma_x)$, all values being normalized to σ_0. In the static case, we optimize Q_3 for fixed Q_1 when Q_1 is not too close to Q_1^{max} which is first determined by maximizing Q_1, other components being free. Conversely, for better convergence of the codes, Q_1 is optimized for fixed values of Q_3. When using the mixed kinematic code, for example in the first case studied below, q_3 is fixed to 1.0 (or -1.0), q_2 to zero and Q_1 is declared fixed to the desired value. In the following the porosity f is fixed to 0.1 and 0.01.

For validation purpose, the codes are first applied to the isotropic hollow sphere problem (e.g. with von Mises matrix as a particular case of the orthotropic one), and then to the problem of a Hill matrix with spherical and oblate cavities. The static model is discretized in a mesh with 13 layers of 12×12 prisms, i.e., 26,208 tetrahedrons. In the kinematic case the mesh is defined by up to $17 \times 17 \times 17$ prisms, i.e., 68,782 tetrahedrons in the anisotropic tests. With one processor core, the static problem runs in about 5000 seconds on a recent Apple Mac Pro, using MOSEK with one processor core; the best refined kinematic mixed problem is solved in 4500 seconds when the classical method of [15] needs at least five times more CPU times: this better efficiency of the mixed approach was a bit unexpected, and pleasant surprise… Indeed, mixed and classical kinematic methods were verified to give very close optimal results when using the same mesh and the von Mises criterion, with a rigorous admissibility confirmation by post-analysis of the two optimal solutions.

4.1. Application to the hollow sphere problem

This subsection is devoted to the case of spherical cavities, for von Mises and Hill matrices. We compare the numerical bounds to the following closed form expression, first derived in [7] for Hill orthotropic matrix and later retrieved in [8]:

$$\sqrt{\frac{3}{2}\left[F(\Sigma_y - \Sigma_z)^2 + G(\Sigma_z - \Sigma_x)^2 + H(\Sigma_x - \Sigma_y)^2\right]} \leqslant \sqrt{\left(1 + f^2\right) - 2f\cosh\left(\kappa\,\Sigma_m^0/\sigma_0\right)} \tag{16}$$

For a given Σ_m^0, the corresponding optimum of $\Sigma_z - \Sigma_x$ is readily obtained by solving with MOSEK the corresponding conic problem with the cone defined by (16) and the linear constraint $\Sigma_x + \Sigma_y + \Sigma_z = 3\Sigma_m^0$.

4.1.1. Case of a von Mises matrix

The (isotropic) von Mises case corresponds to $F = G = H = 1/3$, $L = M = N = 1$ which leads to $\kappa = 3/2$ and allows to recover the classical Gurson criterion from (16). In Fig. 2 are compared the corresponding optimal values of $\Sigma_z - \Sigma_x$ to the results of the present static and kinematic codes.

For isotropic 3D loadings, it can be noted that the Gurson (black) value becomes located between the 3D bounds, as expected since the Gurson value is the exact corresponding solution. It is worth noting also that the present 3D results

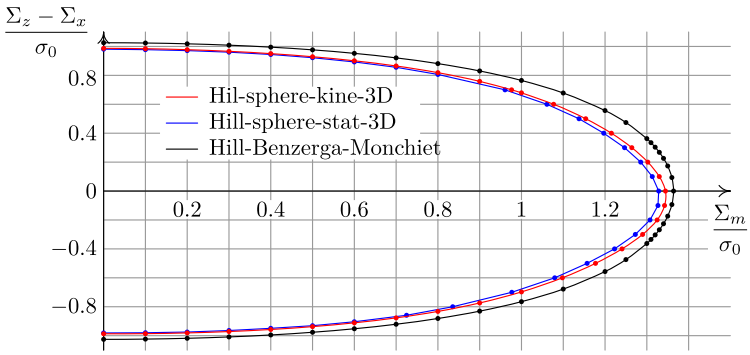

Fig. 3. Spherical void, Hill matrix: comparison with the criterion of Benzerga and Monchiet, $f = 0.1$.

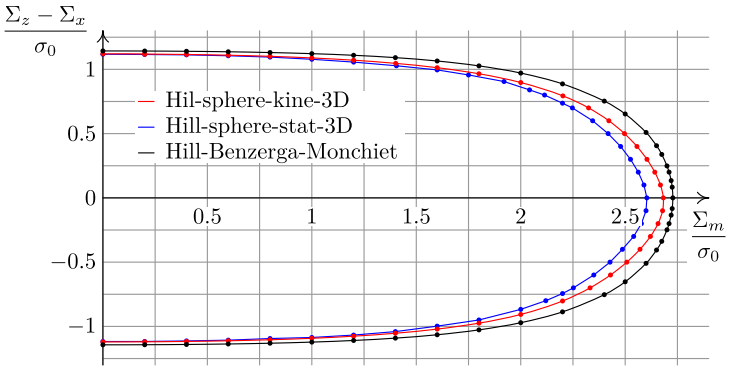

Fig. 4. Spherical void, Hill matrix: comparison with the criterion of Benzerga and Monchiet, $f = 0.01$.

are almost symmetrical around the Σ_m-axis, in contrast to those obtained in [14] where the loadings were axisymmetric. Finally, this test confirms that the Gurson criterion is a good approximation of the exact one for spherical voids.

4.1.2. Case of a Hill matrix

Applications to anisotropic matrices required the following parameters whose values are those used in [8] (with another form of the criterion): $F = 0.331$; $G = 0.402$; $H = 0.168$; $L = 3.669$; $M = 1.141$; $N = 2.2$. This gives rise to $\kappa = 1.68806117$. In Figs. 3 and 4 are plotted the results of the present 3D codes and those obtained as above by solving the one-cone programming problem issued from (16). The obtained lower and upper 3D bounds appear here also very close; the theoretical results are less close to these bounds than in the above case, particularly when the macro-stress triaxiality becomes important. It is also noted that the exact solution appears not symmetric in this case. Moreover, the criterion (16) predicts a value slightly greater than the numerical upper bound on the Σ_m-axis, contrasting with the Gurson result in the isotropic case; this prediction results from the fact that the trial velocity fields used in the theoretical studies and which has led to (16) do not contain the exact solution corresponding to the hydrostatic loading. Finally, it is interesting to note that the criterion (16) does not violate the static approach anywhere. To conclude, it can be considered, at least from the present tests, as a rather good approximation of the exact macroscopic criterion.

4.2. Case of a Hill matrix with oblate cavities

We still consider the previous orthotropic matrix obeying to the Hill criterion, but with an oblate void (see Fig. 1), with $a_1/b_1 = 0.2$. In Figs. 5 and 6 the crosses represent the results obtained in the anisotropic case by Monchiet et al. [8]. The form of the 3D results is similar to those obtained in [15] on the same oblate model but with a von Mises matrix. The results of Monchiet et al. in the case of the orthotropic matrix are a bit far from the 3D bounds; this may be undoubtedly due to the trial velocity fields used by these authors and inspired from the isotropic matrix case. To obtain significantly closer 3D bounds, a quadratic variation of the velocity variables should be necessary, as in [20] for plane strain problems; in this way the strain rate interpolation will be similar to that of the stresses in the present static program.

Finally, the search of corrective parameters q_i to the criterion of Monchiet et al. in order to fit the obtained numerical results was not considered in the present paper for the following reasons. First, obtaining as here the optimal $\Sigma_z - \Sigma_x$ for a fixed Σ_m from the parameterized criterion results in solving an optimization problem, even when the q_i parameters are fixed. Second, considering these parameters as additional variables leads to a non-trivial general optimization problem; this needs to develop a specific solver, keeping in mind that the corrected criterion could become non-convex when introducing

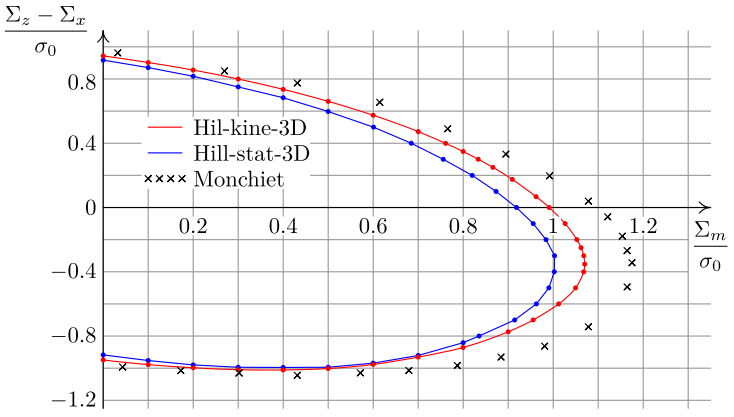

Fig. 5. Oblate void, Hill matrix: comparison with the criterion of Monchiet, $f = 0.1$.

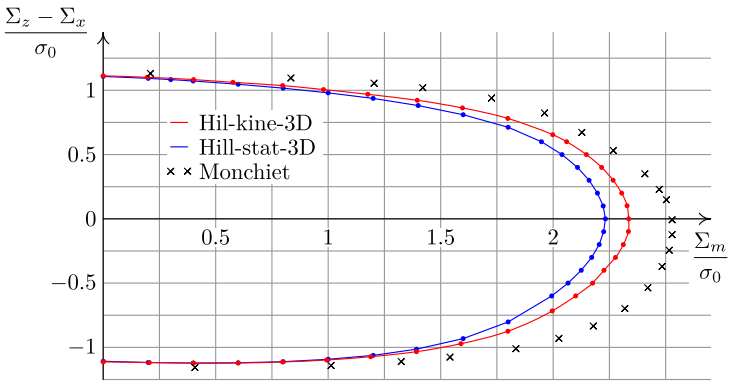

Fig. 6. Oblate void, Hill matrix: comparison with the criterion of Monchiet, $f = 0.01$.

these parameters. Moreover, to be fully valid, this fitting should be searched for more general loadings than the principal stress ones allowed here: this induces to mesh up to a half sphere; keeping also in mind that the corrective set should be tested with several parameters set of the Hill matrix criterion, we can conclude that this would require non-realistic CPU times, at least for the moment. Anyway, to facilitate future control about this mechanical problem with oblate voids, we give in Appendix A almost all the values of the coordinates of Figs. 5 and 6.

5. Concluding remarks

The main purpose of this Note was to assess some theoretical approximate criteria recently available in the literature concerning the hollow sphere or spheroid (confocal) with a Hill orthotropic matrix. To this end, the existing static codes for von Mises matrices (see [15]) have been readily extended to this anisotropic context. In order to obtain the corresponding upper bounds with discontinuous meshes, an original kinematic mixed formulation has been developed and implemented. This allows to avoid the complexity of the classical kinematic approach as regards the indispensable discontinuity surfaces. The resulting mixed code appears better conditioned and robust, allowing to enhance very refined meshes solved with reasonable CPU times. Moreover, both static and kinematic codes can be rapidly adapted to problems involving another classical matrix criterion, and less classical ones (for instance the Mises–Schleicher criterion), by modifying only the criterion part common to both codes. Finally, the character of strict lower and upper bound 3D results has allowed also to quantify the influence of the approximations used by the authors of the theoretical formulations that have been assessed.

Both static and mixed codes have been applied to the hollow sphere problem with, first, a von Mises (isotropic) matrix and then with a Hill matrix. The von Mises test shows very close lower and upper bounds and confirms that the Gurson criterion is a very good approximation of the exact one. In the case of a Hill matrix with spherical voids, the common expression of [7] and [8] can be also considered as a good approximation of the exact criterion, but to a lesser extent than previously. Finally, in the hollow spheroid problem with oblate void, the corresponding Monchiet et al. criterion appears too far from the numerical bounds, owing to the two-component velocity fields considered by these authors. A way to improve this analytical criterion is to consider a larger class of velocity fields. Investigation of particular cases such as cylindrical voids in the Hill orthotropic material may constitute a first step in this research direction.

Appendix A. Tables of MEF values – Hill matrix with oblate voids

Table 1
Results of present MEF kinematic and static approaches for a Hill matrix with oblate void; form factor: $a_1/b_1 = 0.2$; porosity: $f = 0.1$ and 0.01.

Hill matrix, oblate void – $f = 0.1$				Hill matrix, oblate void – $f = 0.01$			
Static		Kinematic		Static		Kinematic	
Σ_m/σ_0	$(\Sigma_z - \Sigma_x)/\sigma_0$	Σ_m/σ_0	$(\Sigma_z - \Sigma_x)/\sigma_0$	Σ_m/σ_0	$(\Sigma_z - \Sigma_x)/\sigma_0$	Σ_m/σ_0	$(\Sigma_z - \Sigma_x)/\sigma_0$
0.0	0.91731	0.0	0.94384	0.0	1.10793	0.0	1.11265
0.1	0.87088	0.1	0.90254	0.4	1.07246	0.40165	1.08327
0.2	0.81699	0.2	0.85555	0.8	1.01677	0.79753	1.03686
0.3	0.75057	0.3	0.79959	1.0	0.98005	1.17621	0.96888
0.4	0.68336	0.4	0.73536	1.2	0.93705	1.39610	0.92219
0.5	0.59753	0.5	0.66071	1.4	0.88130	1.59695	0.86280
0.60077	0.5	0.6	0.57427	1.6	0.81005	1.79838	0.78106
0.68462	0.4	0.7	0.4726	1.8	0.71240	1.99812	0.65472
0.75573	0.3	0.76102	0.39912	1.94787	0.6	2.05988	0.60024
0.82001	0.2	0.83348	0.30028	2.03917	0.5	2.14780	0.49992
0.87304	0.1	0.90923	0.175	2.10814	0.4	2.21550	0.39983
0.91844	0.0	0.99114	0	2.15959	0.3	2.26647	0.30017
0.95561	−0.1	1.02662	−0.1	2.19690	0.2	2.30470	0.20002
0.98409	−0.2	1.05262	−0.2	2.22239	0.1	2.32858	0.10165
1.00307	−0.3	1.06797	−0.3	2.23234	0.0	2.33562	0.0
1.00255	−0.4	1.06774	−0.40049	2.22443	−0.1	2.33451	−0.09863
0.99041	−0.5	1.04981	−0.50017	2.20467	−0.2	2.31175	−0.20027
0.96265	−0.6	1.01231	−0.59995	2.17125	−0.3	2.27689	−0.30064
0.91442	−0.7	0.95564	−0.69960	2.12480	−0.4	2.22576	−0.40067
0.83531	−0.8	0.90007	−0.77341	2.06619	−0.5	2.17518	−0.50018
0.8	−0.84112	0.79973	−0.87124	1.99340	−0.6	2.10005	−0.59963
0.7	−0.92105	0.7	−0.93081	1.8	−0.80222	1.99608	−0.71622
0.6	−0.96846	0.6	−0.97674	1.6	−0.93169	1.79865	−0.87439
0.5	−0.99417	0.5	−1.00223	1.39222	−1.01424	1.59016	−0.97129
0.4	−0.99544	0.4	−1.01077	1.2	−1.06228	1.39222	−1.03356
0.3	−0.99427	0.3	−1.00947	1.0	−1.09271	1.18916	−1.07255
0.2	−0.97956	0.2	−0.99719	0.8	−1.11132	0.79745	−1.11356
0.1	−0.95231	0.1	−0.97767	0.4	−1.12219	0.40178	−1.12213
0.0	−0.91731	0.0	−0.94892	0.0	−1.10793	0.0	−1.11265

References

[1] A.L. Gurson, Continuum theory of ductile rupture by void nucleation and growth. Part I: Yield criteria and flow rules for porous ductile media, J. Eng. Mat. Technol. 99 (1977) 2–15.
[2] M. Gologanu, J.B. Leblond, Approximate models for ductile metals containing non-spherical voids – case of axisymmetric prolate ellipsoidal cavities, J. Mech. Phys. Solids 41 (11) (1993) 1723–1754.
[3] M. Gologanu, J.B. Leblond, G. Perrin, J. Devaux, Approximate models for ductile metals containing non-spherical voids – case of axisymmetric oblate ellipsoidal cavities, J. Eng. Mat. Technol. 116 (1994) 290–297.
[4] M. Gologanu, J.B. Leblond, G. Perrin, J. Devaux, Recent extensions of Gurson's model for porous ductile metals, in: P. Suquet (Ed.), Continuum Micromechanics, Springer-Verlag, 1997.
[5] M. Garajeu, P. Suquet, Effective properties of porous ideally plastic or viscoplastic materials containing rigid particles, J. Mech. Phys. Solids 45 (1997) 873–902.
[6] V. Monchiet, E. Charkaluk, D. Kondo, An improvement of Gurson-type models of porous materials by using Eshelby-like trial velocity fields, C. R. Mecanique 335 (2007) 32–41.
[7] A.A. Benzerga, J. Besson, Plastic potentials for anisotropic porous solids, Eur. J. Mech. A Solids 20 (2001) 397–434.
[8] V. Monchiet, O. Cazacu, E. Charkaluk, D. Kondo, Macroscopic yield criteria for plastic anisotropic materials containing spheroidal voids, Int. J. Plast. 24 (2008) 1158–1189.
[9] S.M. Keralavarma, A.A. Benzerga, A constitutive model for plastically anisotropic solids with non-spherical voids, J. Mech. Phys. Solids 58 (2010) 874–901.
[10] A. Benzerga, J.B. Leblond, Ductile fracture by void growth to coalescence, Adv. Appl. Mech. 44 (2010) 169–305.
[11] P. Francescato, J. Pastor, B. Riveill-Reydet, Ductile failure of cylindrically porous materials. Part I: Plane stress problem and experimental results, Eur. J. Mech. A Solids 23 (2004) 181–190.
[12] J. Pastor, P. Francescato, M. Trillat, E. Loute, G. Rousselier, Ductile failure of cylindrically porous materials. Part II: Other cases of symmetry, Eur. J. Mech. A Solids 23 (2004) 191–201.
[13] M. Trillat, J. Pastor, Limit analysis and Gurson's model, Eur. J. Mech. A Solids 24 (2005) 800–819.
[14] P. Thoré, F. Pastor, J. Pastor, Hollow sphere models, conic programming and third stress invariant, Eur. J. Mech. A Solids 30 (2011) 63–71.
[15] F. Pastor, D. Kondo, J. Pastor, Numerical limit analysis bounds for ductile porous media with oblate voids, Mech. Res. Comm. 38 (2011) 350–354.
[16] F. Pastor, D. Kondo, Assessment of models accounting for voids shape effects on ductile behavior: A conic programming limit analysis approach, submitted for publication.
[17] MOSEK ApS C/O Symbion Science Park, Fruebjergvej 3, Box 16, 2100 Copenhagen ϕ, Denmark, email: info@mosek.com, 2011.
[18] R. Hill, A theory of yielding and plastic flow of anisotropic solids, Proc. R. Soc. Lond. Ser. A 193 (1948) 281–297.
[19] F. Pastor, Résolution par des méthodes de point intérieur de problèmes de programmation convexe posés par l'analyse limite, Thèse de doctorat, Facultés universitaires Notre-Dame de la Paix, Namur, 2007.

[20] F. Pastor, E. Loute, J. Pastor, M. Trillat, Mixed method and convex optimization for limit analysis of homogeneous Gurson materials: A kinematical approach, Eur. J. Mech. A Solids 28 (2009) 25–35.
[21] J. Salençon, Théorie de la plasticité pour les applications à la mécanique des sols, Eyrolles, Paris, 1974.
[22] J. Salençon, Calcul à la rupture et analyse limite, Presses des Ponts et Chaussées, Paris, 1983.
[23] F. Pastor, E. Loute, Solving limit analysis problems: an interior-point method, Comm. Numer. Methods Engrg. 21 (11) (2005) 631–642.
[24] D. Radenkovic, Q.S. Nguyen, La dualité des théorèmes limites pour une structure en matériau rigide-plastique standard, Arch. Mech. 24 (5–6) (1972) 991–998.